An Analysis of Wind Direction and Horizontal Wind Component Fluctuations over Complex Terrain

K. H. PAPADOPOULOS AND C. G. HELMIS

Laboratory of Meteorology, Department of Applied Physics, University of Athens, Athens, Greece

G. T. AMANATIDIS

National Center for Scientific Research "Demokritos" Institute of Nuclear Technology and Radiation Protection, Athens, Greece

(Manuscript received 22 July 1991, in final form 21 October 1991)

ABSTRACT

Based on an extensive wind dataset over complex terrain, the commonly used small-angle approximation $\sigma_v \approx \sigma_\theta V$ is studied and found to overestimate over all wind speeds and σ_θ values observed. This should be anticipated due to the assumptions necessary to derive the approximation. Overestimation (of 10%–30%) is also observed in the small σ_θ range. The three parameters involved are further discussed to gain better understanding of the behavior of the approximation under different conditions. The standard deviation of wind direction σ_θ is shown to vary inversely with wind speed not only under stable, but also under convective conditions, reaching a site-dependent constant value at high wind speeds. The dependence of the ratio of the mean longitudinal wind component to the scalar mean wind speed on wind speed and σ_θ is examined, as well as that of the relevant standard deviations (σ_u, σ_{V_a}). While the former obtains small values in the high-σ_θ, or low-wind range, or both, estimated values of the latter justify equivalence of σ_u, σ_{V_a} under most conditions. Finally, the effects of wind speed and σ_θ on σ_v are examined.

1. Introduction

The wind-direction standard deviation σ_θ constitutes one of the principal estimators of the horizontal diffusing ability of the atmospheric boundary layer. During the usually unstable daytime conditions a maximum is attained. Toward the evening, lower values are measured, while nighttime σ_θ is influenced by wave activity, mesoscale eddies imposed by the terrain features and meandering. Under stable conditions σ_θ varies inversely with wind speed over both flat (Joffre and Laurila 1988; JL hereafter) and complex terrain (Hanna 1980; Etling 1990; Leahey et al. 1988). Additionally, JL found the same behavior also to be valid for unstable conditions. Computation of the wind-direction standard deviation is not straightforward as for other scalar quantities, because of the circular distribution of wind direction values and crossover effect. Therefore, several algorithms incorporating certain assumptions have been presented for handling with the problem (Verrall and Williams 1982; Ackermann 1983; Nelson 1984; Yamartino 1984; Turner 1986).

The standard estimators for the mean value of the wind vector's magnitude are the scalar mean and the vector mean wind speed, to be defined below. Let V_i and D_i be the magnitude and direction, respectively, of the instantaneous wind vector and define the x axis to be along the east–west component of the wind and the y axis along the south–north. Then, if n observations of V_i, D_i are obtained over some selected period of time (the sampling duration) (Mori 1986), the following are defined:

(i) scalar-mean wind speed

$$V_a = \frac{1}{n} \sum V_i \quad \text{and} \tag{1}$$

(ii) vector-mean wind speed

$$V_v = (V_x^2 + V_y^2)^{1/2}, \tag{2}$$

where

$$V_x = \frac{1}{n} \sum V_{xi} = \frac{1}{n} \sum V_i \sin D_i \tag{3}$$

$$V_y = \frac{1}{n} \sum V_{yi} = \frac{1}{n} \sum V_i \cos D_i. \tag{4}$$

The vector-mean wind direction D_v is defined as

$$D_v = \tan^{-1}(V_x / V_y). \tag{5}$$

The instantaneous wind components parallel and perpendicular to the mean wind direction are u_i (lon-

Corresponding author address: Dr. C. G. Helmis, University of Athens, Laboratory of Meteorology, Department of Applied Physics, 33 Ippokratous, 10680 Athens, Greece.

gitudinal), v_i (lateral), respectively. The mean value of u_i is the mean longitudinal wind component u, which equals the vector mean wind speed, provided D_v is used as the estimator of mean direction.

Similarity theory provides relations for the standard deviations of the longitudinal, lateral, and vertical wind components (σ_u, σ_v, and σ_w, respectively). Quite often u and V_a, as well as their standard deviations, are used interchangeably in application of similarity formulas without distinction between them.

Assuming small values of σ_θ, the standard deviation of the lateral wind component σ_v can be approximated by the product $\sigma_\theta V$, where V is either of the estimators for mean wind speed. This approximation is widely used for estimation of σ_θ or σ_v, depending on which of these is readily available. Yamartino (1984), using a limited dataset created with a Gaussian random number generator, discussed the overpredictions of σ_θ estimated by σ_v/V_v for $\sigma_\theta > 40°$.

In this study σ_θ is computed by Yamartino's estimator, while the vector-mean direction is used for estimating mean direction (therefore, u, V_v are equal). The validity of $\sigma_v \approx \sigma_\theta V$ over complex terrain is tested for a wide range of wind speeds and σ_θ values, particularly in the small σ_θ range. The dependence of σ_θ on wind speed under daytime, nighttime, and transition conditions is presented. The differences between u and V_a and σ_u and σ_{V_a} in relation to wind speed and σ_θ are examined. Dependence of σ_v on wind speed and σ_θ is also provided.

2. Observation site—instrumentation

A three-component four-bladed anemometer (distance constant about 2 m, threshold of 0.15 m s^{-1}) is used for the current analysis. The anemometer is operated on the 42-m level of an 84-m meteorological tower (DEMERT) in Athens, Greece (Amanatidis et al. 1990). The tower lies on the foot of the 1024-m-high Hymettos Mountain, which traverses the eastern edge of the Athens urban area along the north–south direction. The base of the tower is 283 m above the mean sea level. The ground around the tower is stony with bushes 50 cm high. There are some trees on the periphery. The roughness length z_0 has been computed from neutral wind profiles to be 1.1–1.6 m, independent of season.

The three outputs of the anemometer, corresponding to the three components of the wind V_{yi}, V_{xi}, and w_i are sampled at a 1-Hz frequency and conversed to the longitudinal u_i, lateral v_i, and vertical w_i wind components. Mean values and second-order moments are stored every 15 min. Hourly values are also directly calculated. Standard deviation of wind direction is calculated according to the Yamartino algorithm, which is more accurate than other estimators of σ_θ (Yamartino 1984; Turner 1986; Mori 1986), especially at great σ_θ values (up to 104°, according to Yamartino). This is important for our analysis since great σ_θ are expected over complex terrain (Hanna 1981).

The data analyzed cover the period between July 1990 and November 1990, giving a total number of 9712 samples of 15-min. duration each. Measurements from a narrow region of 30° were excluded from subsequent analysis to avoid possible interference with the tower structure (Amanatidis et al. 1991).

3. Data analysis and results

a. *Dependence of σ_θ on wind speed*

According to the results presented by Smith and Abbott (1961), Hanna (1981), and Leahey et al. (1988) for stable conditions over rough terrain, σ_θ varies inversely with wind speed. The same behavior was reported by JL over flat terrain for both stable and unstable conditions. The best-fit lines reported in these papers are summarized in Table 1, together with the relevant type of measuring site, atmospheric conditions, measuring height, and sampling duration. The second formula of Table 1 was computed by Etling (1990) based on the measurements of Hanna (1981) and Leahey et al. (1988). Such a behavior, according to $\sigma_v \approx \sigma_\theta V$, implies constancy of σ_v during nighttime conditions, as stated by Hanna (1983), Etling (1990), and others. Figure 1 presents a plot of σ_θ versus V_a for the 5-month period analyzed. Due to the bulk of data, the 15-min σ_θ and mean wind speed were grouped in subsets of V_a (each one covering a 0.5 m s^{-1} wide region), and median values of σ_θ were computed for each one

TABLE 1. Best-fit lines for relations between σ_θ and wind speed.

Equation (σ_θ in degrees)	Height (m AGL)	Type of surface	Conditions	Averaging time	Reference
$\sigma_\theta = 57/V$	10	rough	nighttime (21–06)	1 h	Hanna (1981)
$\sigma_\theta = 45/V$	10	slightly irregular	low speed, stable	1 h	Etling (1990)
$\sigma_\theta = 34/V$	10	foothills	all	1-h median values	Leahey et al. (1988)
$\sigma_\theta = 18/V$ for $V < 5$ m s^{-1} $\sigma_\theta = 4$ for $V > 5$ m s^{-1}	10–15	flat	all	1 h	Joffre and Laurila (1988)

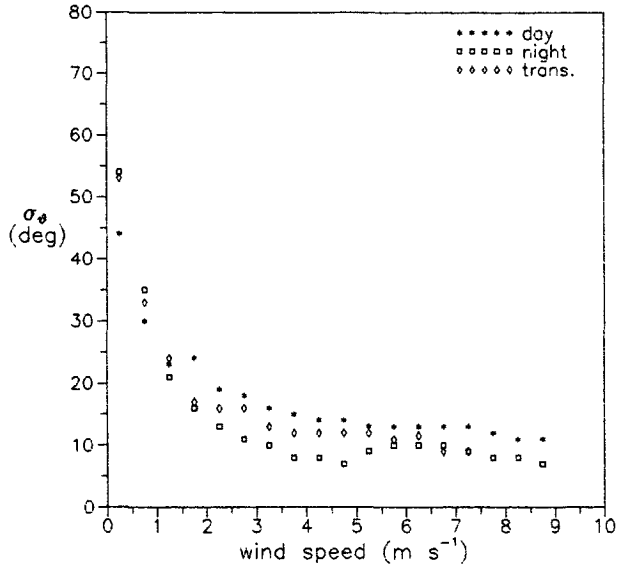

FIG. 1. Median values of 15-min samples of σ_θ values in terms of wind speed for day (stars, 1000–1800 LST), night (squares, 2100–0600 LST), and transition periods (rhomboids, remaining hours).

of the subsets. Points plotted represent these median values for day (1000–1800 LST), night (2100–0600 LST), and transition periods (the remaining hours). The inverse relation between σ_θ and V_a exists for both day and night, suggesting that σ_θ is strongly related to wind speed under both convective and stable conditions. Transition periods exhibit the same pattern. Great variability of σ_θ is observed (not shown here) for low-speed cases with extreme values of 103°. Hanna (1983) also noted a variation of σ_θ between 20° and 100° at wind speeds of 1 m s^{-1}. A leveling of σ_θ accompanied by suppression of variability of σ_θ values is attained for V_a roughly greater than 4 m s^{-1} in accordance with JL's results over flat terrain. Another feature of Fig. 1 is that below 1 m s^{-1} nocturnal values are greater than daytime ones, while the reverse is observed for greater wind speeds. Low wind speeds during the daytime are expected to lead to unstable conditions, while at night they would permit meandering of wind direction. Both these imply big σ_θ, but the reason that nocturnal values exceed the daytime ones is not obvious. For 1 m s^{-1} < V_a < 6 m s^{-1}, daytime σ_θ are greater than nocturnal ones, probably because of enhancement of turbulence due to instability. For V_a > 6 m s^{-1}, as neutral conditions (where turbulence levels are determined by mechanical production) should be approached, nocturnal and daytime σ_θ values converge. Results for transition periods rank in between those for convective and stable conditions. In the 2.5–5 m s^{-1} range, during the night only, lower σ_θ values than for V_a > 5 m s^{-1} are observed. These low values may be attributed to a significantly enhanced frequency of occurrence of winds blowing parallel to the Hymettos Mountain slope. These wind directions have σ_θ lower than other directions (for all wind speeds) possibly because of the presence of the slope that limits wind direction fluctuations.

As σ_θ is known to be affected by the sampling duration selected, in order to be justified in making a comparison with the results of Table 1, the same analysis in Fig. 1 was followed, but using 1-h samples of σ_θ and V_a (Fig. 2). Qualitatively, Figs. 1 and 2 are equivalent, with hourly values being greater than 15-min values. This is expected, as the greater the sampling duration the bigger the scales of turbulence allowed to contribute to the variance. Results, if only nighttime conditions are considered, are also included. The three lines represent the best-fit lines of Table 1 [with the exception of Etling's (1990), which is almost identical to that of Leahey et al. (1988)]. There is general agreement between the present results and those of Hanna (1981) and Leahey et al. (1988) referring to rough terrain and stable conditions. Disagreement with JL's line for flat terrain is expected as σ_θ is enhanced over complex terrain. Their values are 5°–10° smaller for high wind speeds (neutral conditions, when turbulence is determined by surface roughness and wind shear). The reader should keep in mind that our measuring height is significantly greater than those of Table 1. However, similarity theory predicts (Hanna 1981) that during neutral conditions σ_θ is given by the formula

$$\sigma_\theta = \frac{\sigma_v}{V} = \frac{0.8}{\ln(z/z_0)}, \qquad (6)$$

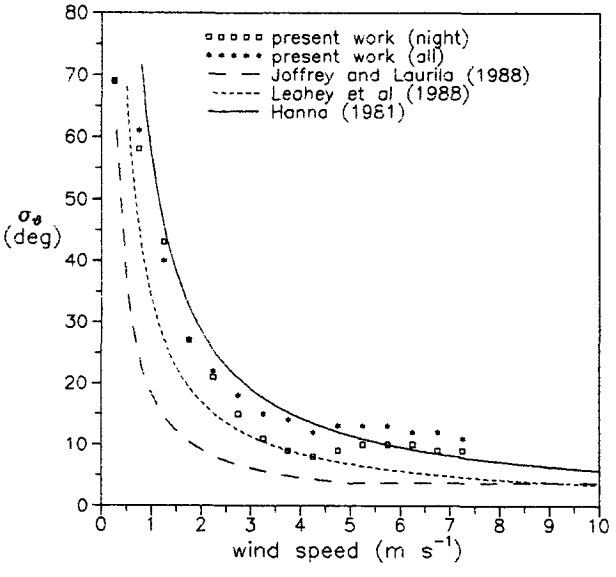

FIG. 2. Median values of 1-h samples of σ_θ values in terms of wind speed under both stable and convective conditions (stars) and under stable conditions only (squares, 2100–0600 LST). The lines represent best-fit lines proposed by Hanna (1981; solid), Joffre and Laurila (1988; long dashed), and Leahey et al. (1988; short dashed). Best-fit lines are summarized in Table 1.

(V is any of the vector- or scalar-mean wind speed) based on the assumption of horizontal homogeneity.

Application of (6) with $z = 42$ m and $z_0 = 1.1$ or 1.6 yields an estimated σ_θ value of 13° and 14°, respectively. The mean value of σ_θ for wind speeds exceeding 6 m s^{-1} was computed to be 12° with a standard deviation of 3°, in agreement with (6).

b. *Comparison of* V_a *and* u *and of relevant standard deviations* σ_{V_a} *and* σ_u

In estimating turbulence intensities and other relevant parameters, the standard deviations of longitudinal (σ_u), lateral (σ_v) wind components, and that of the wind speed (σ_{V_a}) are required.

Mori (1986) showed that V_v and V_a are close to each other, their difference growing with σ_θ and turbulence intensity, and presented several relations between the ratio V_v/V_a and σ_θ. One of the relations (based on Yamartino's work) that was found to match our results better is given here,

$$\frac{u}{V_a} = \exp\left(-\frac{1}{2}\sigma_\theta^2\right), \tag{7}$$

and is valid when fluctuations in wind speed and wind direction are uncorrelated and D_i are normally distributed.

Joffre and Laurila (1988) claim equality of V_a, u, provided that lateral turbulence intensity $I_v = \sigma_v/u$ is small compared to unity.

Figure 3 shows the dependence of the ratio u/V_a on wind speed and σ_θ based on the 15-min samples. Points represent median ratios for bands of V_a values 0.5 m s^{-1} wide (squares) or for bands of σ_θ values 5° wide (stars). The solid line is (7). As theoretically expected, u is lower than V_a through all the range of σ_θ and V_a encountered in this study. For $\sigma_\theta < 10°$, the mean longitudinal component is almost equal to the scalar-mean wind speed. According to Fig. 3, differences greater than 10% are to be expected for $\sigma_\theta > 30°$. Despite the scatter of points above 50° (where the amount of data is rather limited), a tendency for reduction of the u/V_a ratio is indicated. Big σ_θ values are encountered at high turbulence intensities where JL's requirement for equivalence of u with V_a is violated. Indeed, Fig. 3 shows that at these conditions u may well be less than $V_a/2$. The present results follow (7) up to $\sigma_\theta = 30°$. In the high σ_θ region, the assumptions for (7) to be valid are possibly improper, leading to the deviations from these experimental results. If only wind speed is considered, it is seen that for $V_a > 2$ m s^{-1} u is less than 5% smaller than the scalar mean wind speed. At strong winds, mechanical production of turbulence prevails and I_v attains a minimum. Bigger values of I_v are produced under light-wind convective conditions, while under stable conditions the standard deviations increase again, becoming extremely variable (Panofski and Dutton 1984). For $V_a < 2$ m s^{-1}, where the majority of big σ_θ occur, deviations grow up to 20%.

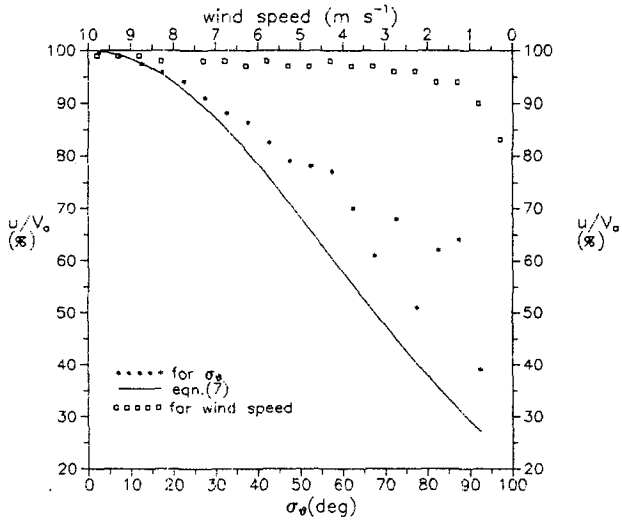

FIG. 3. Relation between ratio of mean longitudinal wind component u to scalar-mean wind speed and wind speed (squares) and σ_θ (stars). The solid line is (7).

In view of these results one could expect equivalence of V_a and u (except, perhaps, close to the rough surface where high turbulence levels are expected) for wind speeds exceeding 2 m s^{-1}. However, if σ_θ exceeds the limit of 20°–30°, u is much lower than V_a, while at $\sigma_\theta < 20°$ u is 1%–5% smaller than V_a. It could also be expected that when strong winds (>10 m s^{-1}) prevail u and V_a should be equal.

In several studies there does not seem to exist a distinction between σ_u and σ_{V_a} or the relevant turbulence intensities I_u and I_{V_a}. Figure 4 is the analog of Fig. 3 for the standard deviations. There is a tendency for σ_u to be slightly greater than σ_{V_a}, but on the average agreement is excellent, the differences being less than 5%. In contrast to Fig. 3 the effect of σ_θ and of V_a on the ratio of the standard deviations is small. For wind speeds greater than 1 m s^{-1} σ_u is within 1% of σ_{V_a}, while below that limit the ratio drops to 96%. The reason why σ_u is smaller than σ_{V_a} is not obvious. Referring to Fig. 3, it is seen that in the same region the deviation of u from V_a is maximum. When $\sigma_\theta < 15°$ σ_u, σ_{V_a} are equivalent on the average. For bigger σ_θ values, deviations smaller than 5% occur, apparently growing in magnitude as σ_θ increases. Scattering of points for $\sigma_\theta > 80°$ is attributed to the limited number of samples in this region.

c. *Evaluation of the approximation* $\sigma_v \approx \sigma_\theta V_a$ *(or* $\sigma_v \approx \sigma_\theta u$*)*

It would be of interest to locate the assumptions necessary to derive the approximation $\sigma_v \approx \sigma_\theta V_a$ or $\sigma_v \approx \sigma_\theta u$.

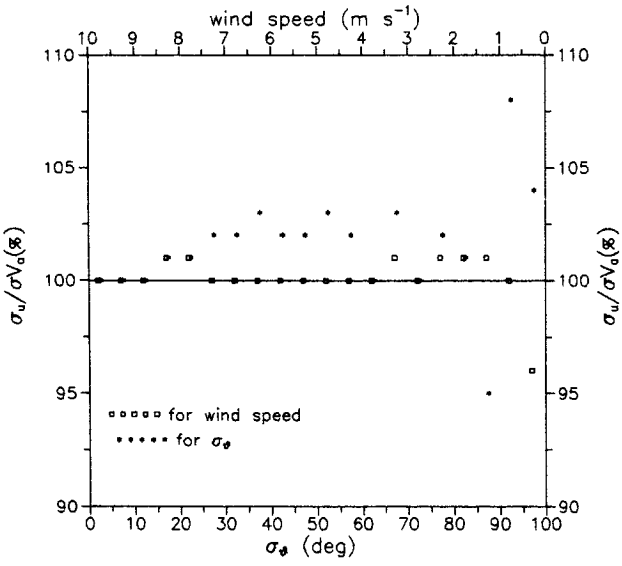

FIG. 4. As for Fig. 3 for the standard deviations.

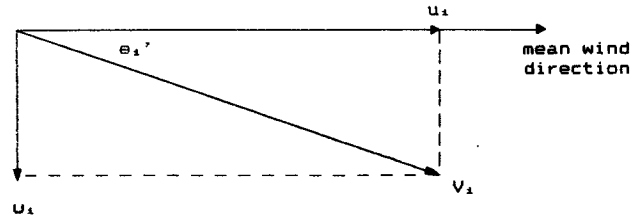

FIG. 5. Geometric representation of instantaneous wind vector, lateral and longitudinal wind components, and mean direction.

In Fig. 5, V_i is the magnitude of the instantaneous wind vector that forms an angle θ_i', with the mean direction derived for the sampling duration under consideration; u_i is the instantaneous longitudinal component, and v_i is the lateral one. Clearly, the rms value of θ_i' is the standard deviation of wind direction. Assuming that (i) θ_i' values are sufficiently small and (ii) V_i is steady in magnitude ($V_i = V_a$) through the sampling duration and/or fluctuations of direction and wind speed are noncorrelated (horizontal homogeneity is satisfied), then

$$\theta_i' \approx \tan\theta_i' = v_i/u_i \tag{8a}$$

$$\theta_i' \approx \sin\theta_i' = v_i/V_i \quad (\theta_i' \text{ in radians}). \tag{8b}$$

Solving (8b) for v_i and applying assumptions (i) and (ii),

$$\theta_i' V_i \approx v_i \rightarrow \text{var}(\theta_i' V_i) \approx \text{var}(v_i)$$

$$\rightarrow V_a^2 \,\text{var}(\theta) \approx \text{var}(v) \rightarrow$$

$$\sigma_\theta V_a \approx \sigma_v. \tag{9}$$

Similarly, if the tangent approximation is preferred,

$$\sigma_\theta u \approx \sigma_v. \tag{10}$$

Mathematically, the sine approximation is more precise. Equation (9) is widely used for estimation of either σ_θ or σ_v, depending on which of the two is readily available.

Over complex terrain, all the prementioned assumptions are questionable and most possibly invalid.

Using 15-min samples of σ_θ, σ_v, V_a, and u and averaging the $\sigma_\theta u$, and $\sigma_\theta V_a$ values in 0.1 m s^{-1} wide regions of measured σ_v, Fig. 6 was constructed. Equation (9) leads to overestimation of σ_v. Overestimation for (10) appears smaller; however, at high σ_v greater scatter is observed.

Table 2 includes the mean-bias error (MBE), the root-mean-square error (rmse), and the linear correlation coefficient r for the approximations expressed by (9) and (10) for three groups of V_a and totality. Equation (9) has a lower rmse and a higher MBE than (10). Both are positively biased. A remarkable reduction of MBE and rmse is observed as wind speed increases. According to Figs. 1 and 2, high wind-speed conditions are characterized by low σ_θ values and the small angle approximation used for extraction of (9) and (10) is more justified. Additionally, (9), which as stated is mathematically more precise, has a considerably greater correlation coefficient, .88 against .68 for (10). It is again seen that as wind speed increases, r increases (note that the data in the high wind speed range are less than those in the low and medium range). As (9) is used more at various studies, in the following we will concentrate on this. In Table 2 the linear correlation coefficient r_h between σ_v and $\sigma_\theta V_a$ is also com-

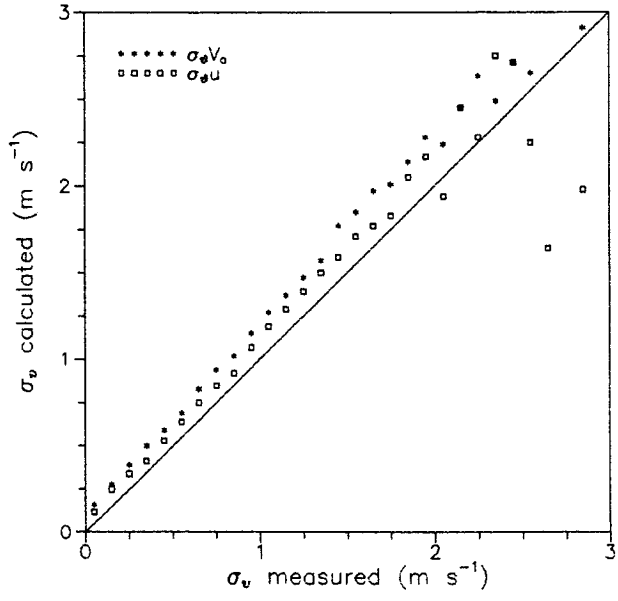

FIG. 6. Mean calculated values of σ_v according to (4) and (5) (stars and squares, respectively) versus measured σ_v values.

TABLE 2. Statistics for the approximations (9) and (10). MBE—mean-bias error, rmse—root-mean-square error, r—correlation coefficient for 15-min samples, r_h—as r for 1-h samples, and N_{15}—number of 15-min samples.

	$\sigma_\theta V_a$				$\sigma_\theta u$			
	MBE	rmse			MBE	rmse		
	(m s^{-1})		r	r_h	(m s^{-1})		r	N_{15}
$V_a \leq 3$ m s^{-1}	0.21	0.37	.82	.71	0.14	0.47	.37	4634
3 m s^{-1} $< V_a \leq 6$ m s^{-1}	0.15	0.28	.90	.84	0.08	0.35	.35	4164
$V_a > 6$ m s^{-1}	0.14	0.19	.96	.98	0.03	0.23	.41	914
All	0.18	0.32	.88	.71	0.10	0.40	.68	9712

puted for hourly samples. The hourly dataset is obviously one-quarter of the 15-min dataset. Again, a remarkable value (.98) of correlation is noticed for high wind speeds.

Overestimation of σ_v by use of the approximation (9) could be in principle expected: an assumption made was that fluctuations of wind speed and wind direction are independent and that wind speed is steady in magnitude ($V_i = V_a$ through the sampling duration). Then,

$$\text{var}(\theta_i' V_i) = V_a^2 \,\text{var}\theta. \qquad (11)$$

But if these fluctuations are not completely independent, as would be expected over a nonhomogeneous complex terrain, then the aforementioned variance should be reduced by an amount analogous to the covariance of wind direction and wind speed fluctuations. Ignoring the covariance provides a potential source of overestimation, as evident in Fig. 6.

Use of $\tan(\sigma_\theta) = \sigma_u/u$, as proposed by Hanna (1983), would blow up for σ_θ approaching 90°, a situation quite usual for low wind speeds (Figs. 1 and 2).

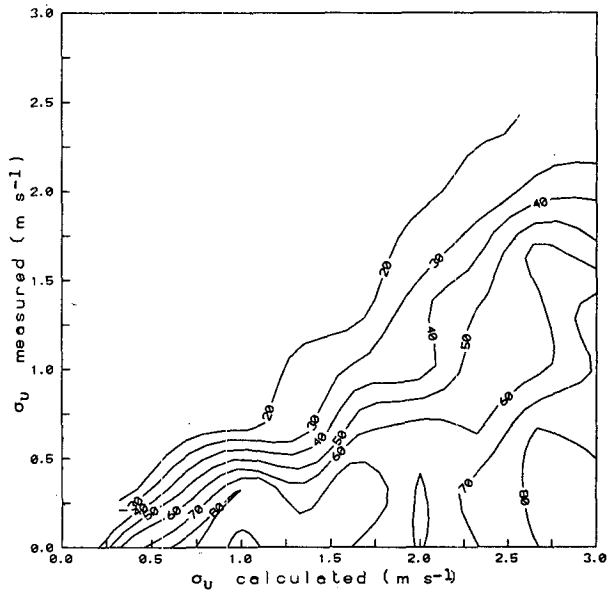

FIG. 7. Contours of σ_θ (deg) values in a (σ_v calculated, σ_v measured) space.

Figure 7 is a more detailed representation of the results of Fig. 6 as it helps clarify the behavior of the approximation in terms of observed σ_θ. For construction of this figure, a grid of σ_θ values in terms of σ_v measured (y axis) and σ_v calculated ($= \sigma_\theta V_a$, x axis) was computed by taking averages of σ_θ for all data points (x_i, y_i) in a properly selected radius around each specified grid point. Size of grid cells and of averaging radius was determined by the requirement to produce a smooth pattern of contours.

A clear ordering of contours is noted: for $\sigma_\theta > 20°$ there seems to be a severe overestimation of σ_v. It is also revealed that for low σ_θ, both σ_v and $\sigma_\theta V_a$ grow along the same contours, which lie close to the $y = x$ line, meaning a linear interdependence. For greater σ_θ values, σ_v seems invariable for values smaller than 0.5 m s^{-1}, while in this region the approximation yields unrealistically big values: overestimations on the order of 100% and more are common. Considerable overestimation was also reported over a plant canopy by Maitani (1983), but for the $\sigma_w \approx \sigma_\varphi V_a$ approximation that is in principle the exact analog of $\sigma_v \approx \sigma_\theta V_a$. In Table 3 we present the statistical properties for (9) in the small σ_θ range, where it is supposed to be valid. For clarity, MBE and rmse are now expressed as percentage errors of observed σ_v. Even in this range the error grows with σ_θ and is not trivial. Relative MBE is 10%–20% (overestimation), and relative rmse is 20%–30%. As shown in the discussion following (11), the overestimation is expected and inherent in the approximation (9) [or (10)]. Therefore, fluctuations of wind speed are always correlated to those of wind direction over complex terrain, as is the site of the present study. The

TABLE 3. Statistics for (9) in the small-σ_θ range. MBE—mean-bias error, rmse—root-mean-square error, r—correlation coefficient (15-min samples), and N—number of 15-min samples.

σ_θ (deg)	MBE (%)	rmse (%)	r	N
0–5	12	20	.97	316
5–10	13	22	.98	1843
10–15	15	29	.98	2641
15–20	20	29	.98	1885
0–20	16	27	.98	6685

same was concluded in Fig. 3 for the big σ_θ range. The correlation coefficient in Table 3 is around .98 through the whole small σ_θ range.

The contours of Fig. 8 reveal that the best performance of (9) occurs for wind speeds greater than 3–4 m s^{-1}, while for low-wind conditions (where σ_θ attains great values, Figs. 1 and 2) the performance seems awkward (see Table 2).

It would be interesting to show the corresponding dependence of σ_v on wind speed and standard deviation of wind direction. Two distinct regions with an intermediate region in between are seen in Fig. 9, which is like Fig. 2 with contours of measured σ_v added. At low wind speeds (<2 m s^{-1}) σ_v attains generally low values (<1 m s^{-1}) that increase as V_a increases. However, at the same region (I), contours are vertical showing that for constant wind speed σ_v is independent of σ_θ. In this region, $\sigma_\theta V_a$ would grow with σ_θ at constant wind speed, leading to the significant errors already seen in Table 2. Note that for $V_a < 3$ m s^{-1} rmse = 0.37 m s^{-1}, while σ_v, in region I of Fig. 8, is in the range of 0.2–0.8 m s^{-1}, resulting to errors on the order of 50%–180%.

On the lower right corner of the diagram, for $V_a > 6$ m s^{-1} (region III), the behavior of σ_v is reversed: contours become horizontal, and for constant σ_θ, σ_v is independent of wind speed. Here σ_v values are sensitive to σ_θ and their range is between 0.4 and 2.2 m s^{-1}. Referring to Table 2 for $V_a > 6$ m s^{-1}, rmse = 0.19 m s^{-1}, thus giving errors on the order of 10%–50%. The slight trend of contours to move slightly downward as wind speed increases in region III permits the product $\sigma_\theta V_a$ to follow satisfactorily the observed values of σ_v.

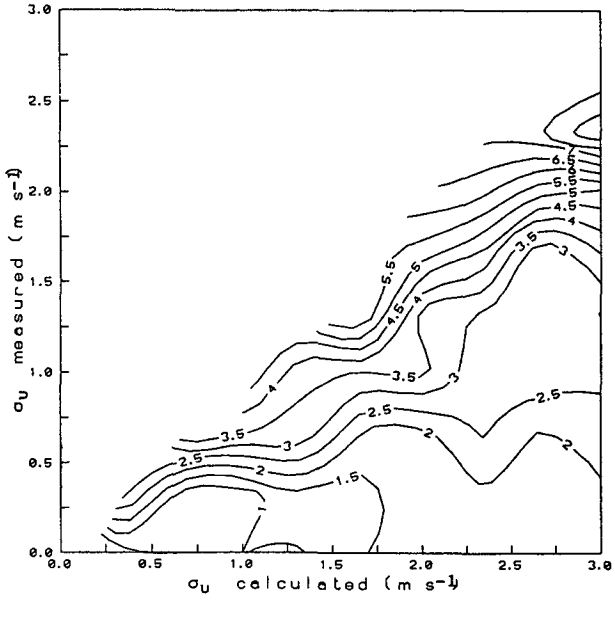

FIG. 8. As for Fig. 8 for wind speed V_a (m s^{-1}).

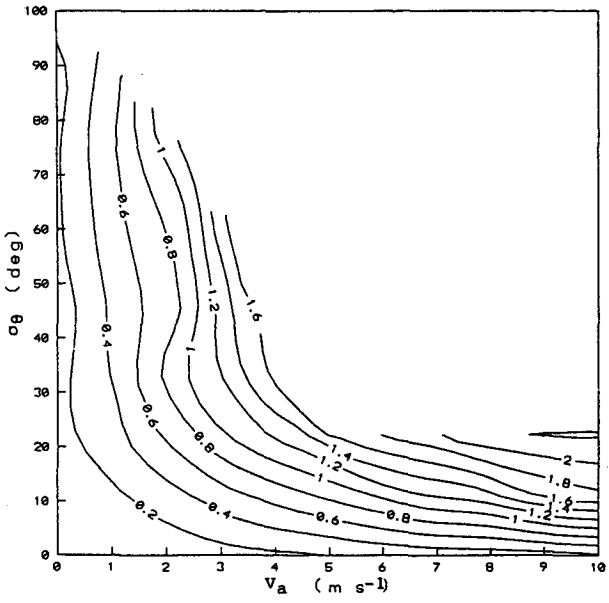

FIG. 9. Contours of measured σ_v (m s^{-1}) values in a (σ_θ, V_a) space.

In region II the behavior of the approximation is intermediate, with errors ranging from 20% to 140%.

In view of these, it is suggested that computation of σ_v is straightforward when possible; otherwise, use of the approximation $\sigma_\theta V_a \approx \sigma_v$ can lead to significant errors up to 180%, especially at low wind speeds and great σ_θ. We note again that low wind-speed conditions are linked to pollution episodes, and an overestimation of σ_v by use of the approximation could lead to great underestimation of pollutant concentrations. However, even in the small σ_θ range, use of (9) would lead to overestimations on the order of 10%–30% that in certain applications might be considered significant.

In order to further test the constancy of nighttime σ_v (Hanna 1983) using 15-min samples, median values of σ_v were calculated in 18 wind-speed regions 0.5 m s^{-1} wide each (Fig. 10). Generally, no constancy is observed. Standard deviation of the lateral wind component increases with wind speed. For wind speeds 2–4 m s^{-1} and mostly for $V_a > 6$ m s^{-1}, σ_v is constant with values of 0.5 and 1.15 m s^{-1}, respectively.

4. Conclusions

Standard deviation of wind direction shows strong dependence on wind speed, varying inversely to it for day, night, and transition periods independently of sampling duration. Big σ_θ values with considerable scatter are observed under low-speed conditions, while for higher speeds σ_θ attains a value determined by surface roughness. A value of about 10°–15° (night and day, respectively) corresponds to our observation site and height in accordance with Hanna's (1980) and Leahey et al.'s (1988) results over complex terrain.

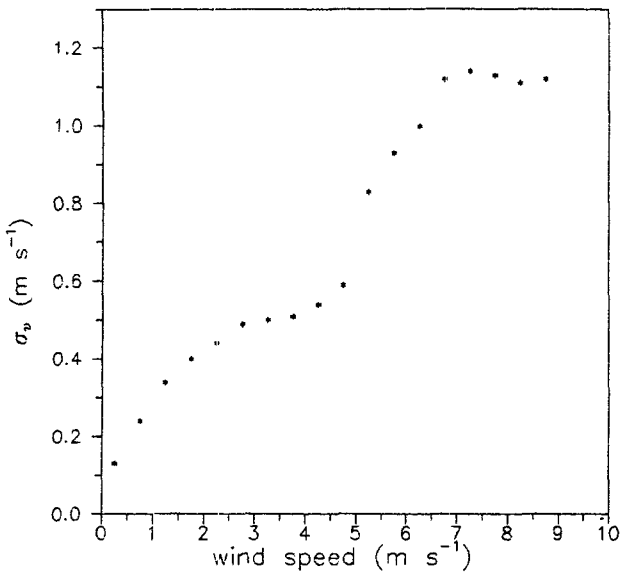

FIG. 10. Median values of σ_v in terms of wind speed for nighttime conditions (for 15-min samples).

Hanna's (1983) proposed best-fit line proves fair during the night, but does not imply constancy of σ_v as stated by the same author. During the night σ_v increases with wind speed, varying between 0.15 and 1.15 m s^{-1}. Additionally, σ_v is shown here to vary with speed at low speed and high σ_θ and to vary with σ_θ at high speeds.

The widely used approximation $\sigma_v \approx \sigma_\theta V_a$ overestimates measured σ_v by 10%–30% for $\sigma_\theta < 20°$ but leads to severe overestimation reaching 180% at greater σ_θ, or low wind speeds, or both. Overestimation is attributed to the assumptions inherent in the approximation. Therefore, direct measurements of both σ_v and σ_θ are required for proper description of turbulence, as the requirement for low σ_θ is not met even over flat terrain when speeds lower than 3–4 m s^{-1} are observed.

Correlation between calculated and measured σ_v becomes higher as wind speed increases, reaching .96. In the small σ_θ range the correlation is .98.

Finally, on the average, standard deviations of the longitudinal component and of wind speed are equivalent. On the other hand, mean longitudinal wind component may be as small as 50% of the scalar-mean wind speed (at least for 15-min samples) when σ_θ exceeds 70° (usually not a very common situation). In the small-σ_θ range, u/V_a approaches unity and the same probably holds for wind speeds greater than 10 m s^{-1}. For lower winds the ratio is 80%–95%.

REFERENCES

Ackermann, G. R., 1983: Means and standard deviations of horizontal wind components. *J. Climate Appl. Meteor.*, **22,** 959–961.

Amanatidis, G. T., B. Synodinou, J. G. Bartzis, D. N. Asimakopoulos, and C. G. Helmis, 1990: The Demokritos meteorological research tower, DEMO 10/90, p. 30. [Available from National Center for Scientific Research 'Demokritos', Athens, Greece.]

——, K. H. Papadopoulos, J. G. Bartzis, and C. G. Helmis, 1992: Evidence of katabatic flows deduced by a 84 m meteorological tower in Athens, Greece. *Bound.-Layer Meteor.*, **58,** 117–132.

Etling, D., 1990: On plume meandering under stable stratification. *Atmos. Environ.*, **24,** 1979–1985.

Hanna, S. R., 1980: Measured σ_y and σ_θ in complex terrain near the TVA Widows Creek, Alabama, Steam Plant. *Atmos. Environ.*, **14,** 401–407.

——, 1981: Diurnal variation of horizontal wind direction fluctuations in complex terrain at Geysers, California. *Bound.-Layer Meteor.*, **21,** 207–213.

——, 1983: Lateral turbulence intensity and plume meandering during stable conditions. *J. Climate Appl. Meteor.*, **22,** 1424–1430.

Joffre, S. M., and T. Laurila, 1988: Standard deviations of wind speed and direction from observations over a smooth surface. *J. Appl. Meteor.*, **27,** 550–561.

Leahey, D. M., M. C. Hansen, and M. B. Scroeder, 1988: An analysis of wind fluctuation statistics under stable atmospheric conditions at three sites in Alberta, Canada. *J. Appl. Meteor.*, **27,** 774–777.

Maitani, T., 1983: Statistics of wind direction fluctuations in the surface layer over plant canopies. *Bound.-Layer Meteor.*, **26,** 15–24.

Mori, Y., 1986: Evaluation of several "single-pass" estimators of the mean and the standard deviation of wind direction. *J. Appl. Meteor.*, **25,** 1387–1397.

Nelson, E. W., 1984: A simple and accurate method for calculation of the standard deviation of the horizontal wind direction. *J. Air Pollut. Control Assoc.*, **34,** 1139–1140.

Panofski, H. A., and J. A. Dutton, 1984: *Atmospheric Turbulence.* Wiley & Sons, 397 pp.

Smith, F. B., and P. F. Abbott, 1961: Statistics of lateral gustiness at 16 meters above ground. *Quart. J. Roy. Meteor. Soc.*, **87,** 549–561.

Turner, B., 1986: Comparison of three methods for calculating the standard deviation of the wind direction. *J. Climate Appl. Meteor.*, **25,** 703–707.

Verrall, K. A., and R. L. Williams, 1982: A method for estimating the standard deviation of wind direction. *J. Appl. Meteor.*, **21,** 1922–1925.

Yamartino, R. J., 1984: A comparison of several "single-pass" estimators of the standard deviation of wind direction. *J. Climate Appl. Meteor.*, **23,** 1362–1366.